Anharmonic interactions and Fermi resonance in the vibrational spectra of alcohols

ARTICLE *in* JOURNAL OF MOLECULAR STRUCTURE · MARCH 2002

Impact Factor: 1.6 · DOI: 10.1016/S0022-2860(01)00762-1

ELSEVIER

Journal of Molecular Structure 605 (2002) 187–198

Journal of
MOLECULAR
STRUCTURE

www.elsevier.com/locate/molstruc

Anharmonic interactions and Fermi resonance in the vibrational spectra of alcohols

N.A. Atamas[a], A.M. Yaremko[b], L.A. Bulavin[a], V.E. Pogorelov[a], S. Berski[c], Z. Latajka[c,*], H. Ratajczak[c], A. Abkowicz-Bieńko[c]

[a]*Department of Physics, Kiev Taras Shevchenko's University,6, Glushkov prospect, Kiev -252127, Ukraine*
[b]*Institute of the Semiconductor Physics of NAS of Ukraine, Prospect Nauki 45, Kiev -252028, Ukraine*
[c]*Faculty of Chemistry, University of Wroclaw, 14, F. Joliot-Curie, 50-383 Wroclaw, Poland*

Received 18 April 2001; revised 12 June 2001; accepted 12 June 2001

Abstract

The vibrational Raman spectra of liquid alcohols ($CH_3(CH_2)_nOH$, $n = 0–3$) were studied experimentally at room temperature in a wide spectral range (1000–4000cm^{-1}). Special attention was paid to investigation of the high frequency region ($\geq$3000cm^{-1}) with the OH-vibration. In addition, DFT calculations of the vibrational spectra were performed. The features of the spectra in the region of $\sim$3000cm^{-1} and the appearance of very broad bands were explained by Fermi resonance as well as very strong coupling between the low frequency vibrational modes and those related to hydrogen bond interactions. © 2002 Elsevier Science B.V. All rights reserved.

Keywords: Raman scattering; Alcohols; Vibrations; Anharmonic interactions; DFT calculations; Fermi resonance; Anharmonicity

1. Introduction

The vibrational spectra of alcohols have been investigated for many years. They are relatively complicated [1] due to their size as well as anharmonic effects giving rise to the mixing of vibrations. Moreover, the occurrence of hydrogen bond vibrations influences the structure of the spectra in the high frequency region.

In the case of alcohols, overtones of vibrations of the CH_3 group are located very close to the fundamental vibrations observed for CH_3 and CH_2 groups and they have the same symmetry which results in Fermi resonance (FR) effects. The intermolecular interaction, responsible for some structural features of condensed phase, is also very important. This feature allows these systems to be used as a model for the study on the formation of mesophases (e.g. the plastic crystals).

The broad range of alcohols in the homologous series ($CH_3(CH_2)_nOH$, $n = 0–3$) gives the possibility for studying the optical properties. Such extensive investigations reveal important information about the vibrational spectra of alcohols. To our knowledge, only for methyl and ethyl alcohol ($n = 0$, 1), have detailed investigation of spectral properties been made. The optical information for the next members in the homologous series are quite poor (see for

* Corresponding author. Tel.: +48-71-320-4440; fax: +48-71-328-2348.
E-mail address: latajka@wchuwr.chem.uni.wroc.pl (Z. Latajka).

PII: S0022-2860(01)00762-1

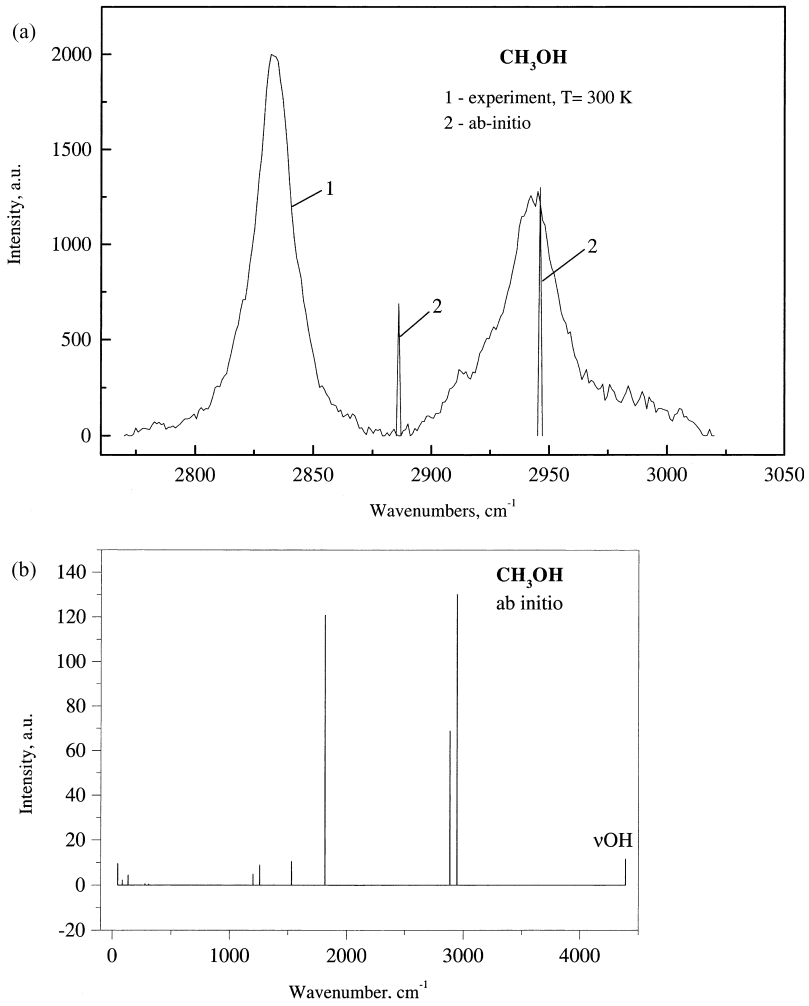

Fig. 1. (a) Experimental Raman spectrum for methyl alcohol (parallel component), curve 1, and theoretically predicted spectrum in the 2750–3100 cm^{-1} region, curve 2. (b) Theoretically predicted spectrum for methyl alcohol in the whole spectral region (0–4500 cm^{-1}).

example Ref. [1]). Therefore, in the present paper, we performed experimental and theoretical investigations for the first few of alcohols in the homologous series to explain the changes in the spectrum along with the increasing number of substituted CH_2 groups. In order to understand the experimental Raman spectra we have performed DFT calculations of the vibrational spectra of several alcohols. It should be noted that the DFT calculated results correspond directly to the gas-phase experimental data. However, the theoretically calculated spectra are used in this paper for qualitative comparison and assignment of bands. Thus, it is anticipated that used level of and model for calculations is satisfactory for this purpose. Furthermore, we studied the influence of anharmonic interaction and FR effect on the band shape in the high frequency region (2900–3500 cm^{-1}).

Special attention was devoted to the position and shape of the band associated with the coupled OH and low frequency vibrations. In order to obtain the unperturbed anharmonic OH frequency we fitted the predicted curves to experimental ones to obtain the anharmonic constants.

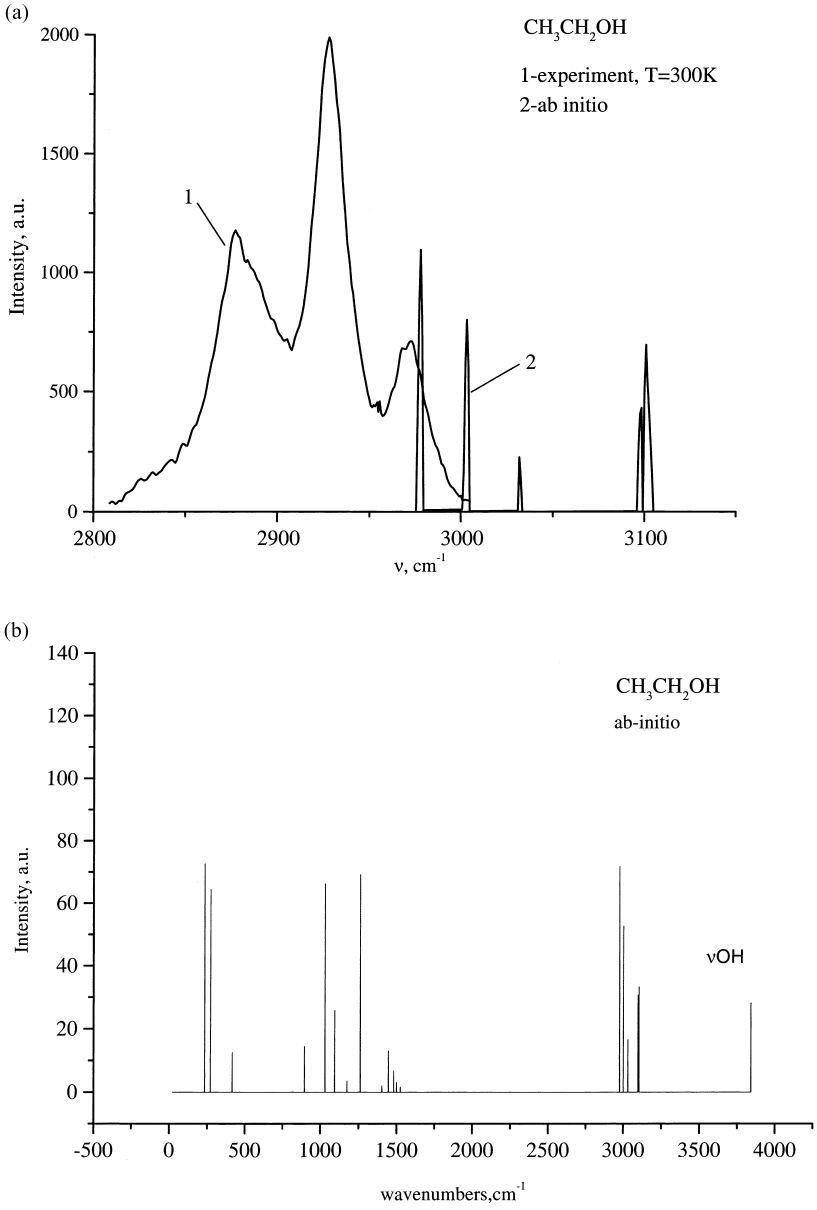

Fig. 2. (a) Experimental Raman spectrum for ethyl alcohol (parallel component), curve 1, and theoretically predicted spectrum in the 2750–3100 cm^{-1} region, curve 2. (b) Theoretically predicted spectrum for ethyl alcohol in the whole spectral region (0–4500 cm^{-1}).

2. Methods

2.1. Experimental technique

The Raman scattering spectra were recorded on a special set up based on the Spectrometer DFS-24. As the source of the light an argon laser generating at $\lambda = 488$ nm was used. The light from the output slit of monochromator was directed to the photomultiplier (FEY-79) and then the intensity was recorded by means of the photon-counting technique. The applied method gives the possibility to record the bands of

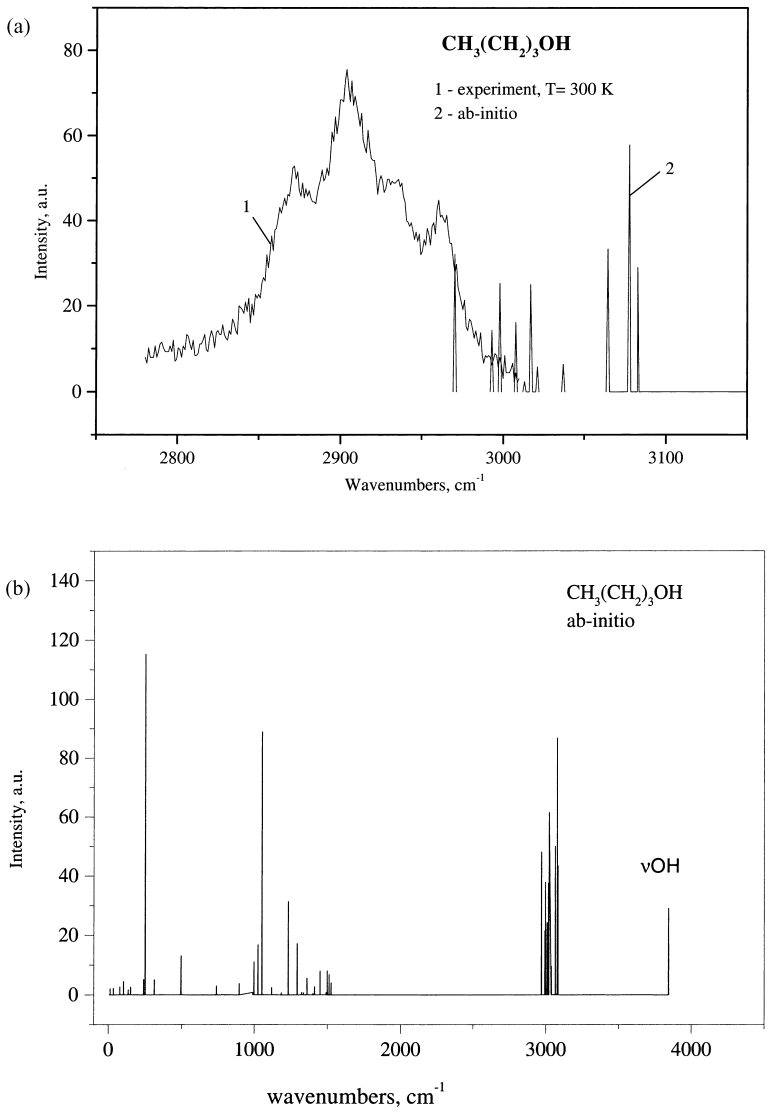

Fig. 3. (a) Experimental Raman spectrum for butyl alcohol (parallel component), curve 1, and theoretically predicted spectrum in the 2750–3100 cm^{-1} region, curve 2. (b) Theoretically predicted spectrum for butyl alcohol in the whole spectral region (0–4500 cm^{-1}).

both isotropic and anisotropic shape and are described by the following expressions:

$$I^*_{\text{anis}}(\omega) = I^*_{\text{vh}}(\omega) = I^*_{\text{hv}}(\omega) + I^*_{\text{hh}}(\omega)$$
$$I^*_{\text{is}}(\omega) = I^*_{\text{vv}}(\omega) - \frac{4}{3} I^*_{\text{vh}}(\omega), \quad (1)$$

where the values denoted by '*' refer to the experimentally recorded bands.

2.2. Quantum chemical calculations

DFT calculations have been performed at the B3LYP level where the Becke exchange functional [5] is coupled with the Lee–Yang–Parr correlation [6]. The standard 6-311++G(d,p) basis set of Frisch et al. [7], has been used. Geometry optimization has been performed under relaxation of all degrees of freedom and the

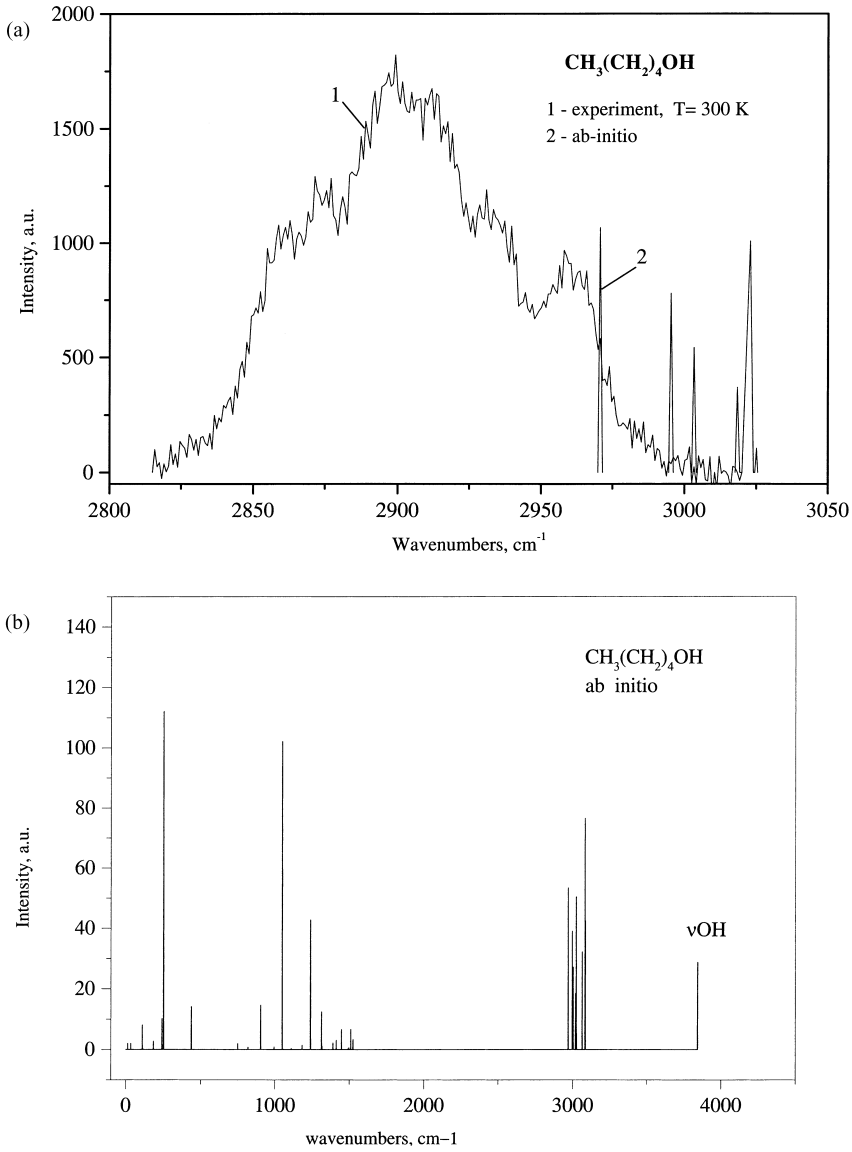

Fig. 4. (a) Experimental Raman spectrum for amyl alcohol (parallel component), curve 1, and theoretically predicted spectrum in the 2750–3100 cm^{-1} region, curve 2. (b) Theoretically predicted spectrum for amyl alcohol in the whole spectral region (0–4500 cm^{-1}).

structural stability was confirmed by the lack of imaginary vibrational frequencies. The vibrational frequencies have been calculated within the harmonic approximation from analytical second derivatives of the energy with respect to the position of the nuclei. The infrared intensities were calculated within the double harmonic approximation from analytical dipole derivatives. All the calculations have been carried out with the Gaussian 94 program package [8].

3. Raman spectra of alcohols

Both isotropic and anisotropic components of the Raman spectra were recorded for all investigated

alcohols at room temperature in the spectral region 1500–3500 cm^{-1}. As the isotropic spectrum is much more interesting than the anisotropic one, the detailed analysis of the former has been done. Special attention was paid to the high frequency region.

For all the studied liquids, bands of relatively complicated shape located in the range from 2800 to 3000 cm^{-1} were observed. The analysis of the Raman spectra presented in Figs. 1–4 shows that with increasing number of atoms the band shape becomes more complicated.

3.1. Methyl alcohol

Methyl alcohol (CH_3OH) is the simplest chemical liquid in the studied homologous series. In the spectral region 2800–3100 cm^{-1} two intense bands with maxima at 2831 and 2942 cm^{-1} were recorded for the parallel component of methyl alcohol (Fig. 1a). These results generally correspond to the data reported previously [1]. The results of DFT calculations are presented in Fig. 1b.

It is seen from Fig. 1a that the band with maximum at 2830 cm^{-1} is symmetrical. On the other hand, the band with a maximum at ≈ 2942 cm^{-1} is unsymmetrical. Moreover, this band is complicated and includes at least two other components. One of them has a clearly marked maximum at 2942 cm^{-1} and the second is the shoulder at about 2831 cm^{-1}. The perpendicular component (not presented in Fig. 1a) has also two maxima at 2831 and 2942 cm^{-1}. The high frequency component is very intense, which is opposite to the results for the parallel case (Fig. 1a).

3.2. Ethyl alcohol

A single, complex spectral band was recorded for parallel Raman scattering component in the spectral region 2800–3100 cm^{-1} (Fig. 2a). The whole contour reveals three bands corresponding to maxima at 2878, 2929 and 2973 cm^{-1}, which is in agreement with the available experimental data [1]. Results of DFT calculations for this molecule are presented in Fig. 2b.

It should be noted that the low frequency component (2878 cm^{-1}) is asymmetrical from the high frequency side. The central band with the maximum at 2929 cm^{-1} is quite symmetrical, whereas the band at 2973 cm^{-1} is characterized by peculiar structure.

3.3. Butyl alcohol

In the case of butyl alcohol, for parallel component in Raman spectra, a four component band (at 2874, 2909, 2935 and 2963 cm^{-1}) was recorded (Fig. 3a) in the high frequency region (2800–3000 cm^{-1}).

The most intense band is observed at 2909 cm^{-1}, with the weakest component at 2963 cm^{-1}. The ratio between the component intensities in the complex band for parallel Raman scattering of butyl alcohol is similar to that obtained for ethyl alcohol.

Ab-initio results are presented in Fig. 3b. A group of bands are located on the background of the very broad (2000–3500 cm^{-1}) unsymmetrical band. This will be further discussed.

For perpendicular Raman scattering component, the central maximum has the highest intensity. A similar effect has been observed for the ethyl alcohol molecule.

3.4. Amyl alcohol

Further complication of the band shape is observed in the case of amyl alcohol $CH_3(CH_2)_4OH$. As can be seen from Fig.4a (parallel Raman scattering component) the structure of the band in the 2800–3000 cm^{-1} spectral region is quite complex and consist of at least six subbands with maxima at 2853, 2873, 2896, 2912, 2941 and 2957 cm^{-1}. The subband located at 2896 cm^{-1} is the most intense, whereas the one at 2912 cm^{-1} is weaker than the band at 2959 cm^{-1}. The theoretically predicted spectrum for amyl alcohol is shown in Fig.4b.

It is very important to emphasize (the detailed discussion will be presented further) that the discussed group of bands (Fig. 4a) is located, as it was observed for butyl alcohol, on the background of a very broad band, demonstrating some structure (1500–3000 cm^{-1}). Such broad bands are due to the effect of strong anharmonic interaction between the OH-vibration and the low-frequency vibrations of the complex molecule. For the perpendicular Raman scattering component the central doublet of subbands has smaller intensity than other bands.

4. Brief theory

As can be seen from Figs. 1a–4a, the Raman

Table 1
The parameters used for the fitting to experimental data. (All *energetic parameters* (ω, χ_i, Γ_i) in relative units, i.e. $\omega_s \equiv \omega_s/2M$, $\Gamma \equiv \Gamma/2M$ etc., where M is the scaling factor. The underlined parameters were varied during the fitting)

	$\underline{\Gamma}$	$\underline{\Gamma_2}$	$\underline{\delta_0}$	d	ω_{comb}	$\underline{\chi_1}$	$\underline{\chi_2}$	Ω_1	Ω_2	M (cm^{-1})
Methyl, RF1	0.3	–	−0.6	–	29	0.01	0.01	1.5	2.5	50
Methyl,RF2	0.1	–	0.18	–	29	0.01	0.01	1.7	2.4	50
Ethyl	0.215	0.17	0.285	0.76	28.9	0.01	0.01	1.2	3.2	50
Buthyl	0.01	–	6	–	29	3	6.2	2.5	4.38	50
Amyl	0.01	–	9	–	29	7	6.1	2.4	2.5	50

spectra of alcohols are quite complicated. We will show that anharmonic interaction of vibrations significantly influences the band shape in the spectrum. To these important effects belong both the Fermi resonance and the strong interaction between the high and low frequency vibrations. The latter effect is especially characteristic for the OH-bond vibrations which produce anomalously broad bands.

4.1. Shape of band

The intensity of Raman scattering (or absorption) of light can be expressed by the Fourier component of the retarded Green function. The spectral profiles taking into account both the Fermi resonance between the fundamental and combination tone and its interaction with the low frequency vibrations are described by the following expressions [2–4]

$$I(\omega) \approx \mathrm{Im}\left[-\sum_{\nu,\mu} d_{n\nu} d^{*}_{n\mu} G^{\nu\mu}_{n}(\omega)\right], \tag{2}$$

where

$$d_{n\nu} = \sum d^{f}_{n}\alpha^{f}_{n\nu}, \qquad d^{f}_{n} = \mu_f d^{0}_{n}, (f = 1, 2),$$
$$\mu_f = [(\delta \pm \delta_0)/2\delta]^{1/2}, \tag{3}$$

Index 'f' denotes to the components of the Fermi doublet; values $\alpha^{f}_{n\nu}, \mu_f$ depend on the conditions of Fermi resonance [3]; d^{0}_{n} characterizes either the dipole moment of the fundamental vibration transition participating in FR (at absorption) or the tensor of Raman light scattering component of molecule; $G^{\nu\mu}_{n}(\omega) = \delta_{\nu\mu} G^{\nu}_{n}(\omega)$ are the Fourier components of Green function; $\delta_0 = \omega_f - 2\omega_2, \delta = (\delta_0^2 + 4\Gamma^2)^{1/2}$; Γ is the anharmonic constant responsible for Fermi resonance.

$$G^{\nu}(\omega) = -i\int_0^{\infty} \mathrm{d}t \exp[i(\omega - \epsilon_{n\nu} + i\gamma_\nu) + g_{n\nu}(t)]. \tag{4}$$

In Eq. (4) the positive value of γ_ν characterizes a natural damping of $\epsilon_{n\nu}$ level for the nth molecule. The function $g_{n\nu}(t)$ has a complex dependence on the lattice frequencies Ω_{sq} and on the coupling constants $\chi^{n\nu}_{sq}$, and is determined as

$$g_{n\nu}(t) = N^{-1}\sum |\chi^{n\nu}_{sq}|^2 \Omega^{-2}_{sq}\{[n_{sq} + 1]\exp(-i\Omega_{sq}t) + n_{sq}\exp(i\Omega_{sq}t) - [2n_{sq} + 1]\}, \tag{5}$$

where n_{sq} is the filling number of vibration with the Ω_{sq} frequency.

In the expressions (2)–(5) the interaction of the high frequency excitations with the lattice phonons are taken into account (which is expressed by the index 'q'). The phonon dispersion, however, is neglected. It causes its transformation into local low frequency excitation, for example the low frequency vibrations of a complex molecule. Therefore, for the usage of the relations (2)–(5), the neglecting of the dependence on the wave vector q is a good approximation in the case of both the lattice phonon frequencies $\Omega_{sq} = \Omega_s$ and the coupling constants $\chi^{n\nu}_{sq} = \chi^{\nu}_{s}$. In addition, bearing in mind the expression for dipole moment transition (Eq.3), one can write:

$$D^{fg}_{n}(0) = \mu_f \mu_g D_0, \chi^{fg}_{sq} = \mu_f \mu_g \chi_{sq}. \tag{6}$$

It is seen now, that the Raman scattering intensity (or the absorption coefficient) e.g. the band shape of spectrum depends on the several parameters describing the interactions: anharmonic constant Γ, coupling constant $\chi^{n\nu}_{sq}$, damping factor γ_ν etc. (see Table 1).

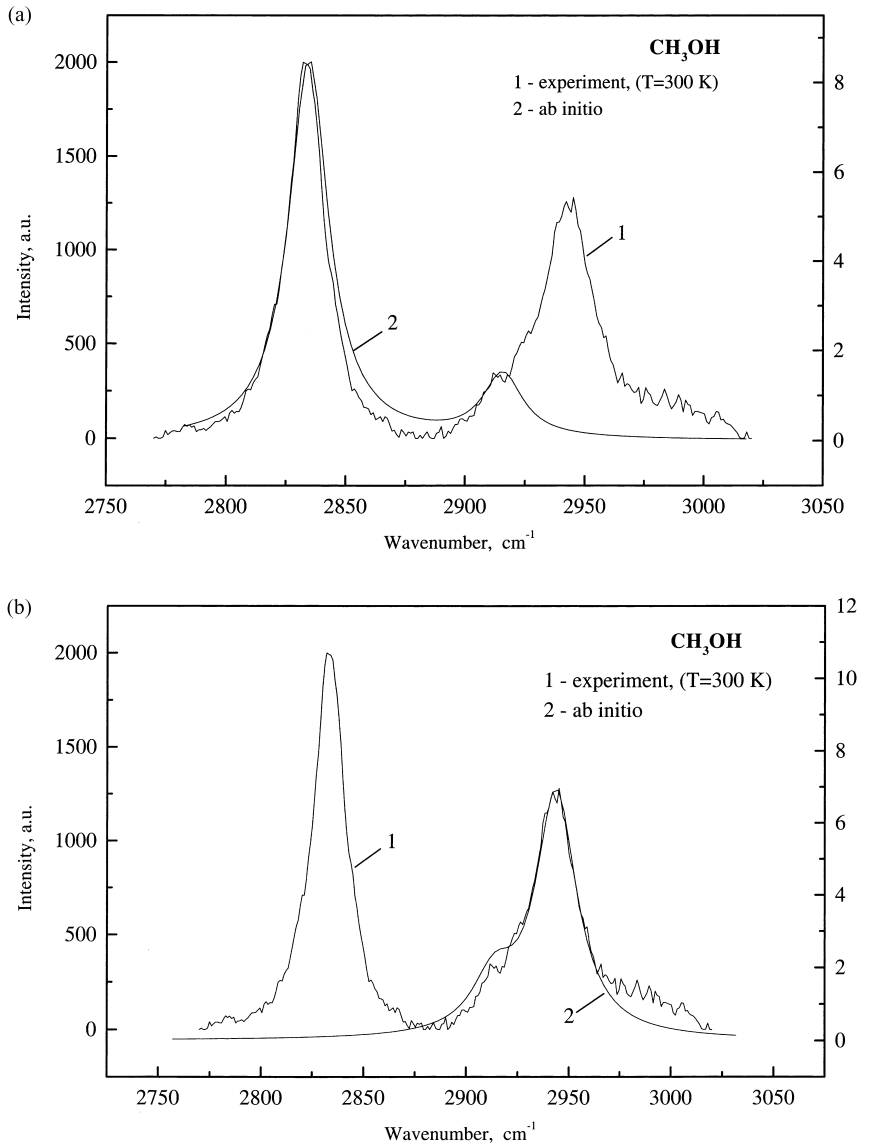

Fig. 5. (a) The comparison between the experimental and theoretical results for Fermi resonance between the overtone and the fundamental band at 2830 cm^{-1} for methyl alcohol. (b) The comparison between the experimental and theoretical results for Fermi resonance between the overtone and the fundamental band at 2940 cm^{-1} for methyl alcohol.

5. Discussion

The analysis of the spectra presented in Figs. 1–4, show their quite complex structure located practically in the same frequency region (2800–3000 cm^{-1}). The more CH_2 groups are added to the alcohol, the more complicated band shape is observed. Such a change in the spectrum is not only due to the changes of the molecular structure, but also the effect of anharmonic interaction of vibrations. In particular, there is a possibility for a strong coupling between the CH- or the OH-vibrations and the low-frequency vibrations of a complex molecule. Therefore, the analysis of the experimental spectra, presented in Figs. 1–4, on the

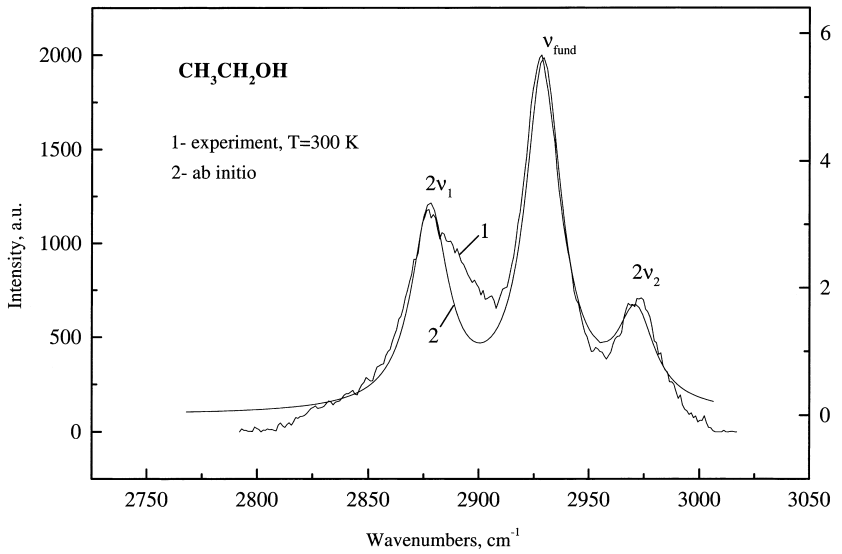

Fig. 6. The experimental spectrum of ethyl alcohol in the region 2800–3050 cm^{-1} (curve 1) along with the theoretically predicted spectrum (curve 2). The two overtones are taken into account.

basis of the approach presented above, seems to be interesting.

5.1. Methyl alcohol

The theoretically predicted frequencies for methyl alcohol along with their intensities are presented in Fig 1b. It can be seen that all vibrations can conditionally be distributed into three principal groups: the low frequency region, $\leq$200 cm^{-1}; the middle frequency region ~1200–1800 cm^{-1}; and high frequency doublet near ~3000 cm^{-1}. The OH vibration arises at relatively high frequency ~4200 cm^{-1}.

It can be noted that both the middle frequency group of bands and the high frequency doublet (Fig. 1b) are in quite good agreement with our experimental results (Fig. 1a) and with the data reported earlier [1]. The quite broad band observed at ~3400 cm^{-1} [1] is related to the OH-vibration.

In our opinion, one more feature observed in the spectrum in Fig. 1a should be discussed. According to the experimental results, an additional band (at ~2900 cm^{-1}) is observed between two intense bands at ~2950 and 2830 cm^{-1}. It arises owing to the Fermi resonance between one of the fundamental vibrations described above and the overtone of ~1450 cm^{-1} vibration. Since the doublet can participate in the Fermi resonance, one should study both possible cases. The results of numerical calculations are presented in Fig. 5a, b. It can be seen that both the experimental and theoretical results are in good agreement with each other; however, the case considered in Fig. 5b seems to be preferable because of the closer proximity of the overtone to the higher frequency (~2950 cm^{-1}) fundamental band.

5.2. Ethyl alcohol

The theoretical results for ethyl alcohol show the 'splitting ' of all frequencies into the three principal groups similarly to the experimental results (Fig. 2a, b): the low frequency region $\leq$500 cm^{-1} with the strong doublet, the middle frequency region ~900–1500 cm^{-1} and high frequency part. It is significant that several intense bands are located in a very narrow part of spectrum (near ~3000 cm^{-1}). The OH band for this molecule is strongly shifted towards higher wavenumbers compared to methyl alcohol (Figs. 1b, 2b). The calculated 'middle' and high frequencies are also in good agreement with known experimental data [1].

In Section 3.2, the existence of the strong triplet of bands at 2974, 2928 and 2873 cm^{-1} was pointed out. Two of them, namely those at 2974 and 2873 cm^{-1},

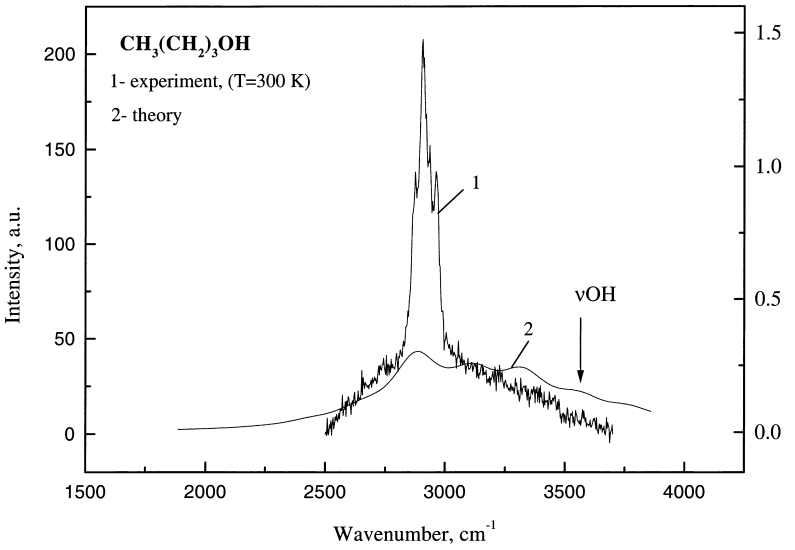

Fig. 7. The experimental spectrum of butyl alcohol in the 2500–3000 cm^{-1} region (curve 1) and the theoretically fitted curve for the antisymmetric OH stretch (curve 2).

can be a result of the Fermi resonance between the fundamental vibration ~2930 cm^{-1} and the overtones of two vibrations at ~1450 and 1470 cm^{-1} [1]. The theoretical results (Fig. 6) show that the experimentally observed triplet of bands is well described by the theoretical formulae (2), though for its low frequency component, the presence of additional band is obviously seen. It is also confirmed by DFT results, Fig. 2b.

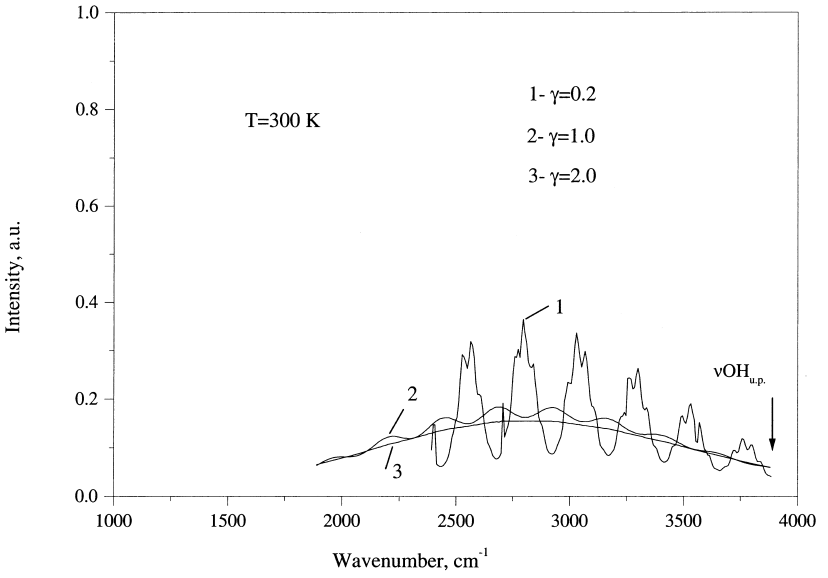

Fig. 8. The theoretically predicted band shapes of the OH stretching vibration strongly coupled with the low frequency vibrations for different damping factor values.

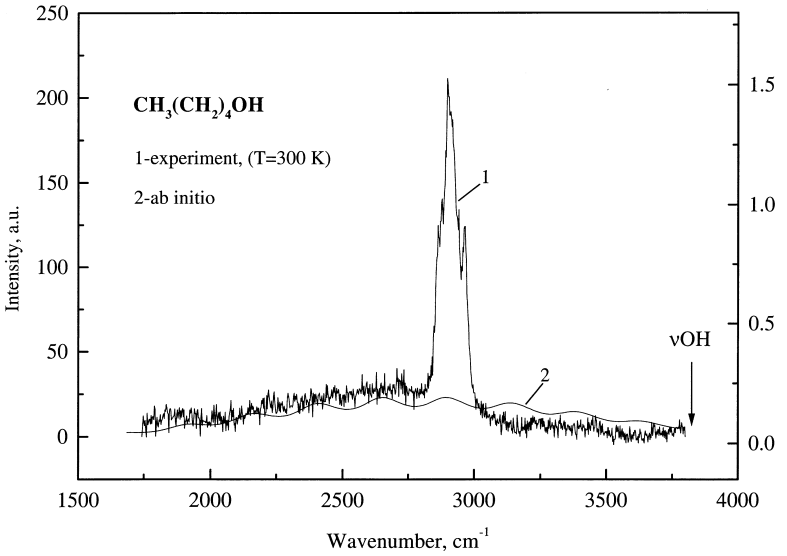

Fig. 9. The experimental spectrum for amyl alcohol in the spectral 1500–3500 cm^{-1} region (curve 1) and the theoretically fitted curve (2) for the broad OH stretching band.

5.3. Butyl alcohol

The theoretically predicted frequencies and intensities are presented in Fig. 3b. The spectrum is divided into three group of bands; however, the number of bands included in each group increases with the increased number of atoms in the molecule. It is clear from Fig. 3b that the analysis of anharmonic interactions between the different components of the group located near 3000 cm^{-1} and the overtones (or combination tones) from the region ~1500 cm^{-1} is very complicated. However, in the case of butyl alcohol there are some changes due to the influence of the hydrogen bond vibration in the ~3000 cm^{-1} spectral region.

It is clearly seen from Fig. 7 that the dense and narrow group of bands located near ~3000 cm^{-1} is placed over the very broad unsymmetrical band. The appearance of such background is due, in our opinion, to the transformation and the shift of the OH-band to the low frequency region because of its strong interaction with the low frequency vibrations of the butyl alcohol molecule [2,3]. (Note that the calculated frequency of the OH-vibration is ~3800 cm^{-1}, Fig. 3b.) To assist understanding this, we present several theoretical curves (Fig. 8), obtained by using the formulae (2)–(5). They show the transformation of the narrow OH-band (denoted by arrow) into a broad structured band. According to our model calculations for the group of alcohols, such change of band shape is the result of the interaction between the OH-vibration and two low frequency vibrations at ~120 and 200 cm^{-1}, respectively. The final band shape depends on the ratio of initial half-width of the OH-vibration, γ, and the meaning of low frequency vibrations, Ω_i, interacting with them. If the half-width is smaller than both frequencies (the case $\gamma = 0.2$ in Fig. 8) the spectrum demonstrates distinct structure (curve 1). If the half-width, however, is bigger than the smallest frequency the structure practically disappears (curves 2 and 3). It should be emphasized, that the increase of both the low-frequency shift and the half-width for the final band along with the growth of the coupling constant, χ_s^{ν}, between OH- and low frequency vibrations is very important.

The description of the broad band in Fig. 7 has been made on the basis of the results presented in Fig. 8. The theoretical curve 2 in Fig. 7 is in good qualitative agreement with the experimental data. The asymmetry of the theoretical curve arises if one of the low frequencies is not 'too small'. In the case of butyl alcohol, the values ~250 and 430 cm^{-1}, obtained by DFT calculations, were consider as the fitting frequencies. It should be noted that the

frequency, ν-OH, unperturbed by anharmonic interaction is found to be equal to $\sim$3600 cm^{-1} which is in quite good agreement with the theoretically predicted value (denoted by arrow in Fig. 7).

5.4. Amyl alcohol

The theoretically predicted spectrum obtained at B3LYP/6-311++G(d,p) level (Fig. 4b) is close to the one calculated for butyl alcohol. The group of intense bands, located near $\sim$3000 cm^{-1}, have practically not changed their position. The same effect is observed for the experimental spectra (Fig. 4a), but for amyl alcohol this dense group of bands is shifted towards higher wavenumbers and significantly broader (2000–3500 cm^{-1}) than for the case of butyl alcohol. One can conclude from the analysis made in Section 5.3 that this band is generated by the OH-vibration very strongly interacting with its own low-frequency vibrations. The theoretical curve 2 in Fig. 9 quite correctly describes the regularities of the experimental spectrum. The fitting frequencies for amyl alcohol are equal to $\sim$185 and 250 cm^{-1}. They are taken from B3LYP/6-311++G(d,p) theoretical calculations.

Since for the experimental spectrum the oscillations are observed, we have used a relatively small damping constant, γ, taking into account the oscillations for the theoretical curve too. That allows us to conclude that the origin of the oscillations in the experimental spectrum are mainly due to many 'phonon' effects arising from strong interaction between the high- and low frequency vibrations of these complex molecules.

On the basis of the obtained results, it can be concluded that the coupling between the OH vibration and the low-frequency vibrations increases in the homologous series. Therefore, very broad bands in the region $\sim$3000 cm^{-1} are observed instead of the usual quite narrow spectral line. So, for butyl and amyl alcohols bands with a large half-width were recorded at $\sim$500 and $\sim$800 cm^{-1}.

6. Conclusion

The theoretical approach adapted in this work, taking into account the strong interaction between high- and low frequency vibrations and the Fermi resonance effect, enables us to understand, at least at the qualitative level, the evaluation of the Raman light scattering spectra recorded for the family of alcohols. It is important to emphasize that there is an increase of the coupling between the OH vibration and the low-frequency modes in the alcohols homologous series. Therefore, instead of the usually observed narrow spectral line, one can find very broad bands in the region $\sim$3000 cm^{-1}. For both butyl and amyl alcohol the bands at $\sim$ 500 and $\sim$800 cm^{-1} with very great half-width are observed.

Acknowledgements

Authors (Z.L., S.B., A.A.-B.) gratefully acknowledge the Wroclaw Supercomputer Center and the Poznan Supercomputer Center for providing time and facilities.

References

[1] B. Schrader, Raman/Infrared Atlas of Organic Compounds, Second Editions, Germany, 1989.
[2] H. Ratajczak, A.M. Yaremko, Chem. Phys. Letters 243 (1995) 348.
[3] D.I. Ostrovskii, H. Ratajczak, A.M. Yaremko, Optics and Spectroscopy 78 (1995) 378.
[4] D.I. Ostrovskii, A.M. Yaremko, I.P. Vorona, J. Raman Spectrosc. 28 (1997) 771.
[5] A.D. Becke, Phys. Rev. A 38 (1988) 3098.
[6] C. Lee, W. Yang, R.G. Parr, Phys. Rev. B 37 (1988) 785.
[7] M.J. Frisch, J.A. Pople, J.S. Binkley, J. Chem. Phys. 80 (1984) 3269.
[8] M.J. Frisch, G.W. Trucks, H.B. Schlegel, P.M.W. Gill, B.J. Johnson, M.A. Robb, J.R. Cheeseman, T.A. Keith, G.A. Peterson, J.A. Montgomery, K. Raghavachari, M.A. Al-Laham, V.G. Zakrevski, J.V. Ortiz, J.B. Foresman, J. Cioslowski, B. Stefanov, A. Nanayakkara, M. Challacombe, C.Y. Peng, P.Y. Ayala, W. Chen, M.W. Wong, J.L. Andres, E.S. Replogle, R. Gomperts, R.L. Martin, D.J. Fox, J.S. Binkley, D.J. Defrees, S.J. Baker, J.P. Stewart, M. Head-Gordon, C. Gonzales, J.A. Pople, GAUSSIAN 94, Gaussian, Inc., Pittsburg, PA, 1995.